Letter

Ultrasonic wave transport in concentrated disordered resonant emulsions

Benoit Tallon [*]
Department of Physics and Astronomy, University of Manitoba, Winnipeg, Manitoba, Canada R3T 2N2

Thomas Brunet
I2M, Université de Bordeaux, CNRS, Bordeaux INP, F-33405 Talence, France

John H. Page [†]
Department of Physics and Astronomy, University of Manitoba, Winnipeg, Manitoba, Canada R3T 2N2

(Received 4 August 2022; revised 31 July 2023; accepted 2 August 2023; published 15 August 2023)

We show how resonant (near-field) coupling affects wave transport in disordered media through ultrasonic experiments in concentrated suspensions. The samples consist of resonant emulsions in which oil droplets are suspended in a liquid gel. By varying the volume fraction of droplets ϕ up to 40%, the limits of the independent scattering approximation are experimentally demonstrated as soon as $\phi > 10\%$. For these concentrated samples, the proximity of resonant scatterers induces a renormalization of the surrounding medium, leading to a reduction in scattering strength. Hence, maximum scattering is reached at an intermediate droplet concentration ($20\% < \phi < 30\%$) where subdiffusive wave transport is observed. These results are very relevant for designing materials for the study of wave transport phenomena such as Anderson localization.

DOI: 10.1103/PhysRevB.108.L060202

Anderson localization of classical waves in three dimensions (3D) has been unambiguously demonstrated more than ten years ago [1]. Such an unusual effect (the halt of wave propagation due to wave interferences) only occurs in strongly scattering heterogeneous media. When the scattering mean free path ℓ_s (the wave attenuation characteristic length due to scattering events) is larger than the incident wavelength λ, interferences are negligible and descriptions based on the independent scattering and ladder approximations are valid to describe wave transport [2]. Under these approximations, the average intensity transport is well described by the diffusion equation [3]. However, when mesoscopic wave interferences are significant, they lead to "subdiffusive" transport or localized signatures such as non-Rayleigh speckle statistics [1,4], wave-function multifractality [5], infinite range correlations [6], and spatial confinement of intensity [1,7], which is also revealed in the dynamics of the coherent backscattering cone [8]. Observations of such mesoscopic phenomena have led to much activity designing new strongly scattering samples for both optics and acoustics experiments [9–16]. In this context, one way to decrease the scattering mean free path is to take advantage of scattering resonances. In acoustics, the mechanical contrast between heterogeneities and the surrounding medium leads to shape resonances [17] (analogous to optical Mie resonances [18]), characterized by large deformations of the scattering inclusions (particles, or droplets in the case of two-fluid media). The wave intensity generated by these deformations is characterized by the cross section σ_s, which is maximized around resonant frequencies. To link the scattering properties of an isolated particle to the global scattering strength of the medium, one can invoke the independent scattering approximation (ISA) [19]. The basic idea of the ISA is to assume that in a diluted medium, a particle will scatter the wave at most once in a scattering sequence. Under this assumption, the scattering can be expressed easily in terms of the cross section $\sigma_s \propto \mathrm{Im}\{f(0)\}$, with $f(0)$ being the forward scattering amplitude for a single scattering event. Thus, the scattering mean free path can be written as $\ell_s = 1/\eta\sigma_s$, with η being the number of scatterers per unit volume.

In this Letter, we show that an increase of the scatterers' concentration η is not necessarily a condition that will lead to a decrease in ℓ_s. By probing both coherent and diffusing ultrasonic wave transport in resonant emulsions, we observe that coupling between nearby resonant scatterers may result in a weakening of the scattering strength of the medium. Our all-fluid suspension of fluorinated (FC40) oil droplets randomly dispersed in a water-based gel matrix constitutes an excellent model system for this study. In diluted emulsions (volume fraction $\phi = 5\%$), we have already observed [11] a strong resonant scattering regime due to high sound speed contrast between oil droplets ($v_1 \equiv v_{\mathrm{oil}} = 0.64$ mm/μs) and the surrounding gel ($v_0 \equiv v_{\mathrm{gel}} = 1.48$ mm/μs). By increasing the concentration, we now show that the scattering strength initially increases but at a slower rate than predicted by the ISA. As the concentration is further increased, we demonstrate that an intermediate concentration between 20% and 30% exists for maximizing the scattering strength. In this concentration range, the scattering is sufficiently strong that the transport becomes subdiffusive and is well described by

[*]Present address: Institut Jean Le Rond d'Alembert, Sorbonne Université - CNRS, 75005 Paris, France.
[†]john.page@umanitoba.ca

 ©2023 American Physical Society

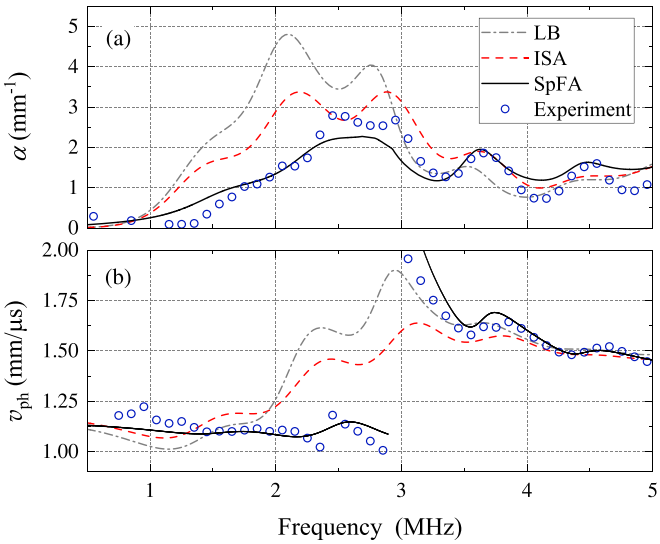

FIG. 1. (a) Attenuation coefficient and (b) phase velocity for $\phi = 25\%$. Experimental data (open circles) are compared to predictions by Lloyd and Berry theory (LB, black dashed-dotted line), the independent scattering approximation (ISA, red dashed line), and the spectral function approach (SpFA, black solid line).

the self-consistent theory of localization. Beyond this concentration, however, the scattering becomes weaker, and simple diffusive transport is again found, with the diffusion coefficient at $\phi = 40\%$ becoming comparable to its value at $\phi = 5\%$. Since the velocity contrast in this emulsion ($v_1 \ll v_0$) is similar to that found in some strongly scattering optical systems, our observation of maximum scattering at a concentration that is less than half that of random close packing may be relevant to finding evidence for the localization of light in 3D [10].

The samples studied here are relatively concentrated all-fluid suspensions ($5\% < \phi \leqslant 40\%$) with a droplet mean radius $\bar{a} = 0.17$ mm. This droplet size allows shape resonances to be observed in the MHz range, as these resonances occur when the wavelength is comparable to the droplet size. Very low droplet polydispersity (∼3%), crucial for studying the influence of resonances on wave propagation [20], was ensured by using microfluidic techniques controlled by robotics [21]. Another advantage of this emulsion system is its almost negligible acoustic dissipation, due to the low viscosity of both FC40 oil and water-based gel. Thus the effects of resonances on wave transport were not obscured by dissipation effects, allowing diffusive wave transport in pulsed experiments to be observed over a long range of times and consequences of mesoscopic interferences to be probed.

Ultrasonic characterization of the samples' basic acoustic properties was performed via ballistic measurements of ensemble-averaged transmitted acoustic wave pulses, as described in detail in Refs. [11,21]. Hence, accurate measurements of both the amplitude attenuation coefficient α and the phase velocity v_{ph} were performed, quantifying the impact of droplet shape resonances on wave propagation as illustrated in Fig. 1 for $\phi = 25\%$. Note that because dissipation is negligibly small, α provides a measure of the scattering mean free path ($\ell_s = \frac{1}{2}\alpha^{-1}$ to an excellent approximation [11,21]).

Figure 1 reveals that predictions based on the independent scattering approximation (ISA) [19], as well as theories such as the Lloyd and Berry model (LB) [22] that include higher-order corrections, do not describe the experimental data well. In these theories, the wave number k of the ballistic wave can be written as

$$k^2 = (k' + jk'')^2 = k_0^2 + \eta\delta_{k_0}, \tag{1}$$

where $k' = \omega/v_{\text{ph}}$, $k'' = \alpha$, and ω is the angular frequency of the incident plane wave. Here, δ_{k_0} is the modification of the wave number in the pure matrix k_0 due to scattering and can be expressed as a function of the amplitude of a wave scattered by an isolated droplet $f(\theta)$,

$$\delta_{k_0} = 4\pi f(0) \quad \text{(ISA)},$$
$$\delta_{k_0} = 4\pi f(0) - \eta\frac{4\pi^2}{k_0^2}\left[f^2(0) - f^2(\pi) + \int_0^{\pi}\frac{df^2(\theta)}{d\theta}\frac{d\theta}{\sin(\theta/2)}\right] \quad \text{(LB)}, \tag{2}$$

where θ is the angle between the directions of the incident and scattered waves. Thus, $f(0)$ and $f(\pi)$ represent the amplitudes of forward and backward scattered waves, respectively. Uncorrelated point scatterers are assumed in the ISA model, making this theory relevant only for dilute media ($\eta \ll 1$). When η increases, the finite size a of scatterers induces spatial correlations (the "hole correction" [23]) included in LB theory.

For a concentrated heterogeneous medium in the intermediate frequency regime ($\lambda \sim a$), waves incident on a given scatterer may include substantial contributions from the waves scattered by nearby scatterers. In this case, the surrounding matrix may be viewed as an effective medium that depends on scatterers' properties [2] and the correction δ depends on the wave number k. Hence, the implicit equation $k^2 = k_0^2 + \eta\delta_k$ needs to be solved. A theory using these concepts is the spectral function approach (SpFA) [2,24]. As shown in Fig. 1, better agreement is found between our experiments and SpFA predictions than between these experiments and the ISA or LB theories.

The scattering concept that is incorporated in the SpFA is illustrated in Fig. 2(a). We calculate the scattering amplitude $f_{\kappa_e}(\theta)$ of the wave scattered by an oil droplet that is coated with the water-based gel and immersed in an effective medium, with wave number κ_e, whose value is to be determined at each frequency ω. The radius of the coating b is expressed as a function of the volume fraction of scatterers $b = a/\phi^{1/3}$ while the presence of the coating enables a multiple scattering contribution from structural correlations between droplets and the matrix to be included. Physically, the properties of the effective medium take into account the effect of this scattering from neighboring particles, resulting in a weakening of the effective contrast between a scatterer and the surrounding matrix. The spectral function may be approximated as

$$S(\omega, \kappa_e) = -\text{Im}\langle G\rangle \approx -\text{Im}\frac{1}{4\pi\eta f_{\kappa_e}(0)}, \tag{3}$$

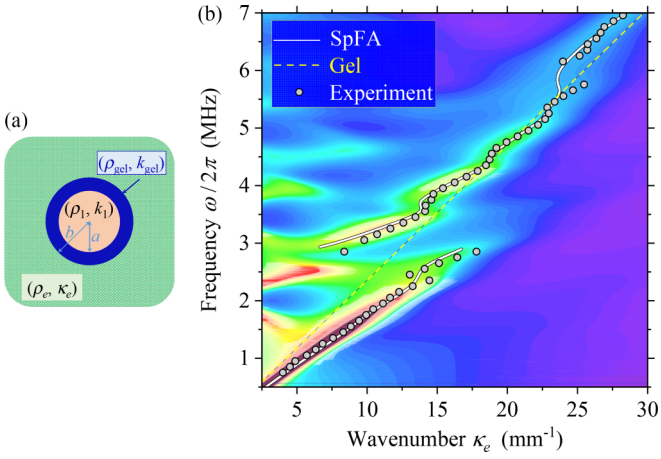

FIG. 2. (a) Illustration of the scattering problem that has to be solved to find the dispersion relation of the quasimodes. A droplet (pale orange) is coated with a layer of gel (blue) and embedded in a uniform medium (textured green) with wave number κ_e. (b) Map of the calculated spectral function $S(\omega, \kappa_e)$ at $\phi = 25\%$. The color scale [from smallest to largest $S(\omega, \kappa_e)$] ranges from purple through dark and light blue, green and yellow to light and dark red. The peak values of $S(\omega, \kappa_e)$ yield the dispersion curve (solid white line, with a black edge), which is compared with the experimental data (solid gray circles, with a black edge). The dispersion line in pure gel (dashed yellow and black line) is also shown.

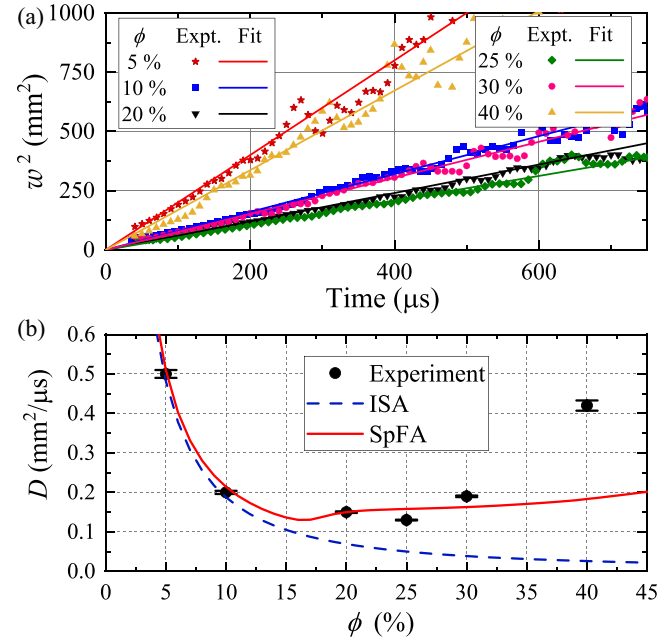

FIG. 3. (a) Transverse width squared $w^2(t)$ for $\rho = 25$ mm, frequency 2.50 MHz, and droplet volume fractions ϕ from 5% to 40%. At this frequency, $w^2(t)$ grows linearly with time, as shown by the straight line fits (solid lines) to the data (symbols). (b) Diffusion coefficient D vs volume fraction ϕ, comparing experimental values (symbols) from the linear fits in (a) with ISA and SpFA predictions (dashed blue and solid red lines, respectively).

where $\langle G \rangle$ is the average Green's function of the effective medium. For each frequency ω, the algorithm scans trial values of κ_e to find the optimum value $\kappa_e = k'$ that gives a maximum of the spectral function $S(\omega, \kappa_e)$ (i.e., the κ_e value corresponding to the least scattering) [2,25]. The maxima of S for all frequencies ω identify the propagating "quasimodes," which have a finite width due to radiative damping. The solutions of Eq. (3) at the peaks of S determine the dispersion curve (Fig. 2) and allow the calculation of the effective phase velocity $v_{ph} = \omega/k'$ as well as the "renormalized" scattering cross section $\sigma_{\kappa_e=k'} = 4\pi\,\mathrm{Im}\{f_{\kappa_e=k'}(0)\}/k_0$, from which we can deduce $\ell_s(\omega) = 1/\eta\sigma_{\kappa_e=k'}$ and $\alpha = 1/(2\ell_s)$. Very good agreement is found, across the entire frequency range, between the calculated dispersion relation of the quasimodes and the experimental data [Fig. 2(b)]. This good agreement persists not only for the phase velocity v_{ph} but also for the attenuation coefficient α, as shown in Fig. 1.

We characterize next the transport behavior of the multiply scattered waves by using the transverse confinement method [1,7]. Using a pointlike source (here a focusing ultrasonic transducer), the acoustic transmission across a slab of emulsion was measured with a needle hydrophone to accurately resolve the position dependence of the multiply scattered wave field along the output surface of the sample [21]. When $\ell_s \gg \lambda$, wave interferences can be neglected, the scattered wave transport is analogous to a random walk process, and the diffusion approximation [3] can be reliably used to describe the transport of energy by the multiply scattered waves. In this case, the transmitted average wave intensity $I(\rho, t)$ has a Gaussian spatial shape (the diffusive halo)

$$I(\rho, t)/I(0, t) = \exp[-\rho^2/w^2(t)], \tag{4}$$

where ρ is the transverse distance with respect to the source (for $\rho = 0$, the source and receiver are aligned on opposite sides of the slab). The squared width of the halo, $w^2(t)$, increases linearly with time, with $w^2(t) = 4D_B t$ depending on the (Boltzmann) diffusion coefficient $D_B = v_E \ell^*$. (Here, v_E and ℓ^* are the energy velocity and transport mean free path, respectively [2].) By contrast, when $\ell_s \approx \lambda$ or smaller, destructive interferences slow down the diffusive wave transport, leading to a nonlinear evolution of $w^2(t)$ [1]. The ultimate limit is Anderson localization, for which the width squared tends to a constant value [1,26] at long times, indicating a trapping of wave energy in the vicinity of the source.

For most frequencies between 1 and 3 MHz, the width squared $w^2(t)$ increases linearly with time, enabling the diffusion coefficient D to be measured as a function of frequency and concentration ($5\% \leqslant \phi \leqslant 40\%$). Figure 3 shows our results at a representative frequency of 2.5 MHz where scattering due to droplet resonances is strong (cf. Fig. 1). Both the slopes of $w^2(t)$ and the values of D vary considerably with concentration, with a minimum in D being found experimentally near $\phi = 25\%$. Even though this minimum in D is not a *direct* measure of maximum scattering strength (which corresponds to a minimum in $k\ell_s$), it does demonstrate that the effects of strong resonant scattering are greatest at this concentration, since resonant scattering is the mechanism that causes both ℓ^* and v_E, and hence D, to be significantly reduced [11,21]. Furthermore, the experimental evidence that the scattering is maximized at an intermediate volume fraction between 20% and 30% is confirmed

by our ballistic measurements, which indicate that $k\ell_s$ is minimized in this concentration range. This behavior contrasts with that observed for suspensions of hard particles (e.g., glass spheres), where the resonances are weaker and the strongest scattering was found for random close packing [3,27].

In Fig. 3(b), we also compare our experimental emulsion data for D with the predictions of the ISA and the SpFA, using calculations similar to those described in Ref. [21]. The relatively good agreement between experiment and the SpFA model for the diffusion coefficient points to the mechanism underlying the observation of maximum scattering around $\phi = 25\%$. When there are very strong scattering resonances, the scattering of waves from nearby scatterers effectively weakens the overall scattering strength relative to what would be predicted in the ISA, an effect that is encapsulated in the model via an approximate effective medium whose properties become closer to those of individual scatterers. As the concentration of scatterers increases, the scattering strength initially increases simply because there are more scatterers, but it then passes through a maximum as the renormalization of the effective medium around each scatterer becomes more pronounced, before decreasing at higher concentrations where D becomes larger again. While the SpFA model captures the overall behavior well, it underpredicts the experimentally observed increase in D at $\phi = 40\%$, likely reflecting a limitation due to approximations in the model.

This evidence for maximum scattering at an intermediate concentration of strongly resonant scatterers motivates a closer investigation of wave transport in this system. By probing the behavior near 2.5 MHz for $20\% \leqslant \phi \leqslant 30\%$, we find evidence of subdiffusive transport at frequencies for which the scattering mean free path is shortest [28]. Figure 4 shows our experimental results for the transmitted intensity $I(\rho, t)$ and width squared $w_\rho^2(t)$ [with $w_\rho^2(t)$ being defined in the same way as $w^2(t)$ in Eq. (4)] at a frequency of 2.43 MHz and at $\phi = 25\%$. The clear difference between our experimental data for $w_\rho^2(t)$ and a diffusive linear evolution (black dashed line) reveals the subdiffusive wave transport in this resonant emulsion. In addition to its nonlinear temporal evolution, the dependence of $w_\rho^2(t)$ on the transverse distance from the source ρ is another characteristic of subdiffusive wave transport, for which the halo deviates from a Gaussian spatial shape [1,7]. Hence, in contrast to the diffusive case (e.g., Fig. 3), it is necessary to insert the subscript ρ in $w_\rho^2(t)$ when the transport is subdiffusive, as in Fig. 4 [7]. These experimental observations of subdiffusive behavior are well described by the self-consistent theory (SCT) of localization [29], which accounts for the renormalization of the diffusion coefficient by interferences and for the resulting spatial dependence of $D(\mathbf{r})$ in finite samples. From the best fit of the SCT to the experimental data, following the approach detailed in Ref. [7], we find that the scattering strength $k'\ell_s$ is only ~5% above its critical value $(k'\ell_s)_c$, below which Anderson localization would be reached. Similar behavior is found for $\phi = 20\%$ and 30%, where $k'\ell_s - (k'\ell_s)_c$ is somewhat larger [see the inset in Fig. 4(b)], but no evidence for subdiffusive behavior is found at concentrations outside this range. Thus, the data in Fig. 4 further support our observations of maximum scattering near $\phi = 25\%$.

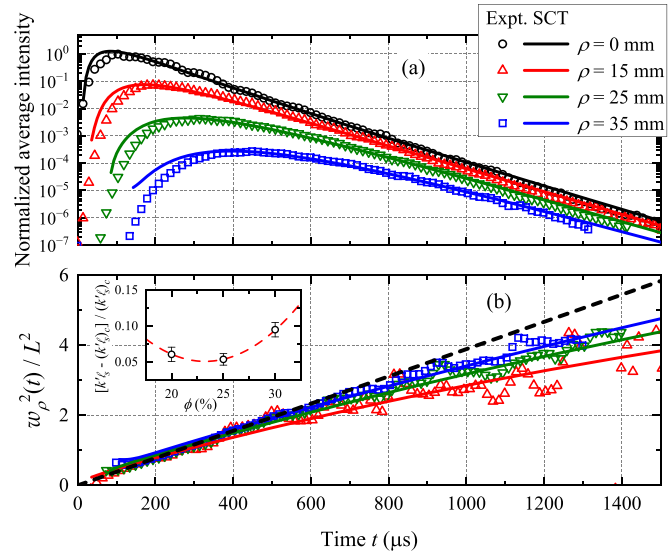

FIG. 4. (a) Temporal evolution of the average transmitted intensity $I(\rho, t)$ for different values of the transverse distance ρ and for a frequency $\omega/2\pi = 2.43$ MHz. The transmitted intensities were measured at the surface of the sample, and are normalized so that $I(0, t)_{\max} = 1$. (b) Corresponding $w_\rho^2(t)/L^2$, where $L = 12$ mm is the thickness of the slab. Experimental data are represented by symbols and SCT predictions by solid lines. The black dashed line represents the linear behavior of $w^2(t)/L^2$ expected for classical diffusion. The inset displays the fraction by which the scattering strength $k'\ell_s$ exceeds its critical value at an Anderson transition, $[k'\ell_s - (k'\ell_s)_c]/(k'\ell_s)_c$ determined by the best fits of the SCT to experiment for $20\% \leqslant \phi \leqslant 30\%$. Note that its variation with ϕ mirrors the behavior of D plotted in Fig. 3. Here, symbols represent the fitted values $[k'\ell_s - (k'\ell_s)_c]/(k'\ell_s)_c$, with the dashed red line being a guide to the eye.

Despite the very strong scattering in our resonant emulsions that is maximized at intermediate droplet concentrations, the Anderson localization transition could still not be reached, motivating the search for other fluid or fluidlike suspensions in which such behavior can be found. Soft matter techniques have great potential for creating suspensions with higher scattering properties, as they allow the design of monodisperse inclusions with controlled sound speeds and even stronger scattering resonances [30,31]. For example, soft porous silicone rubber has a very low sound speed ($v_1 \approx 100$ m/s) [32], resulting in suspensions with scattering strength as high as $k'\ell_{\text{ext}} \approx 0.05$ [33]. Such suspensions are therefore promising candidates once the challenge of fabricating a large number of these spherical particles has been overcome.

In conclusion, our acoustic experiments on emulsions, which may be considered a model system for investigating the effects of resonant scattering on wave transport, show that the scattering strength increases with droplet concentration only up to a certain threshold. Beyond this threshold, due to multiple scattering coupling between nearby resonant droplets, the effective scattering becomes so weakened that the diffusivity actually increases with concentration. This coupling effect manifests itself as a deviation from the ISA and LB theories. However, by taking this effect into

account via a renormalized effective medium surrounding the scatterers, the spectral function approach provides a good overall description of this reduction of scattering strength as concentration increases. For our resonant emulsions, we find that the scattering strength is maximized at an intermediate volume fraction of droplets in the range $\phi \in [20–30]\%$, leading to multiply scattered wave transport with a significant deviation from diffusive behavior that is the most subdiffusive possible in this system [34]. Despite the renormalization effects causing the reduction in effective wave velocity contrast between the surrounding medium and the scatterers, it should be possible to employ soft matter techniques to design new resonant suspensions for which this limitation does not prevent observations of extreme behavior such as Anderson localization. Since the difference in velocities between scattering inclusions and their surroundings is similar for soft matter suspensions in acoustics and typical strongly scattering media in optics, our findings should be relevant to wave transport in a quite wide range of heterogeneous materials.

This work was supported by the LabEx AMADEus (ANR10-LABX-42) within IdEx Bordeaux (ANR-10-IDEX-03-02), i.e., the Investissements d'Avenir programme of the French government managed by the Agence Nationale de la Recherche, and the Natural Sciences and Engineering Research Council of Canada's Discovery Grant Program (RGPIN-2016-06042 and RGPIN-2022-04130).

[1] H. Hu, A. Strybulevych, J. H. Page, S. E. Skipetrov, and B. A. van Tiggelen, Nat. Phys. **4**, 945 (2008).
[2] P. Sheng, *Introduction to Wave Scattering, Localization, and Mesoscopic Phenomena* (Springer, Heidelberg, 2006).
[3] J. H. Page, H. P. Schriemer, A. E. Bailey, and D. A. Weitz, Phys. Rev. E **52**, 3106 (1995).
[4] A. A. Chabanov, M. Stoytchev, and A. Z. Genack, Nature (London) **404**, 850 (2000).
[5] S. Faez, A. Strybulevych, J. H. Page, A. Lagendijk, and B. A. van Tiggelen, Phys. Rev. Lett. **103**, 155703 (2009).
[6] W. K. Hildebrand, A. Strybulevych, S. E. Skipetrov, B. A. van Tiggelen, and J. H. Page, Phys. Rev. Lett. **112**, 073902 (2014).
[7] L. A. Cobus, W. K. Hildebrand, S. E. Skipetrov, B. A. van Tiggelen, and J. H. Page, Phys. Rev. B **98**, 214201 (2018).
[8] L. A. Cobus, S. E. Skipetrov, A. Aubry, B. A. van Tiggelen, A. Derode, and J. H. Page, Phys. Rev. Lett. **116**, 193901 (2016).
[9] A. Lagendijk, B. A. Van Tiggelen, and D. S. Wiersma, Phys. Today **62**(8), 24 (2009).
[10] S. E. Skipetrov and J. H. Page, New J. Phys. **18**, 021001 (2016).
[11] B. Tallon, T. Brunet, and J. H. Page, Phys. Rev. Lett. **119**, 164301 (2017).
[12] J. Haberko, L. S. Froufe-Pérez, and F. Scheffold, Nat. Commun. **11**, 4867 (2020).
[13] A. Goïcoechea, S. E. Skipetrov, and J. H. Page, Phys. Rev. B **102**, 220201(R) (2020).
[14] R. Monsarrat, R. Pierrat, A. Tourin, and A. Goetschy, Phys. Rev. Res. **4**, 033246 (2022).
[15] K. Vynck, R. Pierrat, R. Carminati, L. S. Froufe-Pérez, F. Scheffold, R. Sapienza, S. Vignolini, and J. J. Sáenz, arXiv:2106.13892 [Rev. Mod. Phys. (to be published)].
[16] A. Yamilov, S. E. Skipetrov, T. W. Hughes, M. Minkov, Z. Yu, and H. Cao, Nat. Phys. (2023), doi:10.1038/s41567-023-02091-7
[17] T. Brunet, S. Raffy, B. Mascaro, J. Leng, and R. Wunenburger, Appl. Phys. Lett **101**, 011913 (2012).
[18] G. Mie, Ann. Phys. **330**, 377 (1908).
[19] M. Lax, Rev. Mod. Phys. **23**, 287 (1951).
[20] B. Mascaro, T. Brunet, O. Poncelet, C. Aristégui, S. Raffy, O. Mondain-Monval, and J. Leng, J. Acoust. Soc. Am. **133**, 1996 (2013).
[21] B. Tallon, T. Brunet, J. Leng, and J. H. Page, Phys. Rev. B **101**, 054202 (2020).
[22] P. Lloyd and M. V. Berry, Proc. Phys. Soc. **91**, 678 (1967).
[23] J. G. Fikioris and P. C. Waterman, J. Math. Phys. **5**, 1413 (1964).
[24] X. Jing, P. Sheng, and M. Zhou, Phys. Rev. A **46**, 6513 (1992).
[25] Note that $S(\omega, \kappa_e)$ has to be scanned at constant ω to find the peaks that correspond to an ultrasonic propagation experiment.
[26] N. Cherroret, S. E. Skipetrov, and B. A. van Tiggelen, Phys. Rev. E **82**, 056603 (2010).
[27] M. L. Cowan, K. Beaty, J. H. Page, Z. Liu, and P. Sheng, Phys. Rev. E **58**, 6626 (1998).
[28] These frequencies near 2.5 MHz at which l_s is smallest vary slightly with concentration, because multiple scattering coupling between droplets causes volume-fraction-dependent shifts in the resonant frequencies.
[29] S. E. Skipetrov and B. A. van Tiggelen, Phys. Rev. Lett. **96**, 043902 (2006).
[30] T. Brunet, J. Leng, and O. Mondain-Monval, Science **342**, 323 (2013).
[31] S. Raffy, B. Mascaro, T. Brunet, O. Mondain-Monval, and J. Leng, Adv. Mater. **28**, 1760 (2016).
[32] T. Brunet, A. Merlin, B. Mascaro, K. Zimny, J. Leng, O. Poncelet, C. Aristégui, and O. Mondain-Monval, Nat. Mater. **14**, 384 (2015).
[33] A. Ba, A. Kovalenko, C. Aristégui, O. Mondain-Monval, and T. Brunet, Sci. Rep. **7**, 40106 (2017).
[34] We emphasize that our finding of maximum scattering at an intermediate concentration of strongly scattering resonant inclusions should be a quite universal result, although the exact concentration at which the scattering is maximized will naturally depend on system-specific details such as the multiple scattering coupling between scatterers.